Available online at www.sciencedirect.com
SCIENCE DIRECT®
International Journal of Mass Spectrometry 239 (2004) 147–159
International Journal of Mass Spectrometry
www.elsevier.com/locate/ijms

Proton transfer mass spectrometry studies of peroxy radicals

D. Hanson*, J. Orlando, B. Noziere[1], E. Kosciuch

Atmospheric Chemistry Division, National Center for Atmospheric Research, P.O. Box 3000, Boulder, CO 80305, USA

Received 19 September 2003; accepted 20 July 2004
Available online 1 October 2004

Abstract

A laminar flow reactor coupled to a proton transfer mass spectrometer utilizing $H_3O^+\cdot(H_2O)_n$ cluster ions is described. Experiments involving the Cl-atom initiated oxidation of organic species (cyclohexane, cyclopentane, ethane, methane) were performed in the flow reactor and detection of the peroxyl radicals and other oxidation products are discussed. The detection sensitivities for the RO_2 radicals (R = cyclohexyl, ethyl, and methyl) were estimated. The sensitivities are consistent with a fast rate (coefficient $\sim 10^{-9}$ cm^3 molecule^{-1} s^{-1}) for the proton transfer reaction between many RO_2 species and water-proton clusters. The effect of the presence of water vapor in the ion drift region (IDR) on the detection sensitivity for RO_2 was investigated. The detection of the methyl and ethyl peroxy radical species was adversely affected by water vapor however, that for the cylcohexyl peroxy radical was much less affected. The cyclohexyl- and cyclopentyl-peroxy radicals were reacted with NO and the products so formed were probed with proton transfer from water molecules. Products identified include a wide array of mono-, di-, and tri-functional species containing peroxyl, alcoholic, carbonyl, nitrate, and peroxynitrate functional groups. These products are shown to be in accord with the current state of knowledge on the oxidation of cyclopentane and cyclohexane.

Keywords: Proton-transfer mass spectrometry; Peroxy radicals; Atmospheric oxidation; Ion-molecule reaction

1. Introduction

Proton transfer from water-proton clusters in conjunction with a mass spectrometer (PTr-MS) is a versatile detection scheme for a wide variety of organic compounds in the atmosphere and in other applications [1]. Chemical ionization with water-proton clusters has been studied extensively in the laboratory [1,2]. With respect to atmospheric chemistry, the technique has been used for quantification of organic compounds in ambient air (e.g., [3–7]), for the elucidation of hydrocarbon oxidation mechanisms in chamber systems (e.g., [8–16]); or for kinetics studies of organic peroxy radicals ("RO_2" where R is an organic group) such as CH_3O_2 [17,18], $CH_3CH_2O_2$ [19], and $C_3H_7O_2$ [20]. These initial forays into the use of chemical ionization for the study of peroxy radicals employed ionization conditions (high pressures and low electric fields) such that the water proton clusters were large, i.e., $H^+(H_2O)_n$ with $n > 3$.

Here, we describe two types of experiments. First, organic peroxyls (RO_2) were generated from reaction of Cl with alkanes (methane, ethane, cyclohexane) in the presence of O_2 and the detection sensitivity for these RO_2 species was studied. The affect of water vapor on the detection of RO_2 species was also explored. We also describe the flow reactor where radicals are generated and discuss the design and performance of a new ion drift region (IDR) for a PTr-MS. In the second set of experiments, excess NO was added to the reaction mixtures containing cyclohexyl peroxy or cyclopentyl peroxy radicals, and the resulting oxidation products were detected and interpreted in terms of the atmospheric chemistry of the parent cyclopentane and cyclohexane. The methodology of the kinetic analysis that is needed to understand and quantify some of the data is also presented.

* Corresponding author. Tel.: +1 303 497 1888; fax: +1 303 497 1477.
E-mail address: dhanson@ucar.edu (D. Hanson).
[1] Present address: Marine and Atmospheric Chemistry, Rosenstiel School for Marine and Atmospheric Science, University of Miami, 4600 Rickenbacker Causeway, Miami, FL 33149, USA.

1387-3806/$ – see front matter © 2004 Elsevier B.V. All rights reserved.
doi:10.1016/j.ijms.2004.07.021

2. Experimental

2.1. Radical generation

Radicals were produced in a glass cylindrical flow reactor (inner diameter, 5.0 cm, length 120 cm) connected to a PTr-MS. Four fluorescent lights (40 W each, 122 cm long, UV: 330–360 nm) were aligned axially with the reactor at about 10 cm from its center. Illumination with the UV lights photolyzed a small fraction of the Cl_2, present at 1–10 mTorr levels, producing Cl atoms that quickly reacted with an alkane RH (between 1 and 100 mTorr):

$$Cl_2 + h\nu \rightarrow 2Cl \quad (1)$$

$$Cl + RH \rightarrow HCl + R \quad (2)$$

The alkyl radical, R, added O_2 very rapidly (present at between one and several hundred Torr) to yield peroxyl radicals, RO_2:

$$R + O_2 + M \rightarrow RO_2 + M \quad (3)$$

Trace amounts of NO ([NO] between 10^{10} and 3×10^{12} cm^{-3}) could be introduced into the flow reactor as well to react with peroxyl radicals. For some experiments, water vapor was added to the flow at levels up to 0.5% mixing ratio using the vapor above de-gassed, de-ionized water. The flow reactor was at or near room temperature (there was slight heating due to the lamps, $\Delta T < 10$ K), and total pressure was between 40 and 620 Torr. The majority of the carrier gas was nitrogen with the exception of experiments at high (80% mixing ratio) O_2 levels.

It was found that, with the Cl_2 levels used here, illuminating just a portion (15–20 cm length) of the flow reactor was sufficient for the easy detection of radicals. Thus radicals could be produced in one region and the average reaction time was set by the rate of flow and the distance from the production region to the detector. For experiments where quantitative kinetics were desired, the traditional flow reactor plug flow approximation was employed [21]. The total flow rate (primarily of N_2) was between 1 and 3 sLpm (STP l min^{-1}), which, for typical conditions, results in residence times of a few seconds. In addition to varying the total flow rate and pressure, the residence time could also be set by varying the region of the flow reactor that was illuminated with UV light.

The radical concentrations expected in these experiments can be estimated from the photolysis rate of Cl_2 and the fluence of light from the four lamps. A 10% efficiency for production of UV light from the 40 W lamps would correspond to approximately 4×10^{15} photons cm^{-2} in the center of the flow reactor. A cross section for Cl_2 of 10^{-19} cm^2 molecule^{-1} (the average over the range 330–360 nm) [22] and quantum yield of unity would thus result in a photolysis rate for Cl_2 of $\sim 4 \times 10^{-4}$ s^{-1}. Typical concentrations [Cl_2] of 10^{14} cm^{-3} would thus correspond to a production rate of d[Cl]/d$t \sim 10^{11}$ cm^{-3} s^{-1}. For a typical illumination length of 15 cm and average flow velocity of 5–50 cm/s, radical concentration in the reactor should be in the range of 10^{10} to 10^{11} cm^{-3}. Although this estimate does not take into account the difficulties of collimating the extended light source, the flow velocity radial profile, or radical losses by self-reaction or on the walls, it is in good agreement with the radical concentrations obtained from titration experiments (see below), which gives good confidence in our understanding of these experiments.

Nitrogen was taken from the vapor over liquid nitrogen and O_2 was UHP grade (Scientific Gas Products). Methane (99%) or ethane (99.5%) were admitted into the flow of carrier gas to the reactor via a small leak valve. An estimate of their partial pressure was taken to be equal to the small rise in pressure upon their addition to the flow of gases. For cyclopentane and cyclohexane (both 99+%, Aldrich), the vapor over the liquid held at 273 K was entrained in a flow of N_2 gas. Their abundance was estimated from their vapor pressures [23] and assuming they had saturated the flow. Mixtures of chlorine in N_2 ($\sim$10% and $\sim$1%) were prepared from chlorine (UHP grade, Scientific Gas Products) and N_2. NO was taken from a 22 ppmv mixture in N_2 and its concentration in the flow reactor was calculated from the measured flow of this mixture and the main carrier gas flow. The partial pressure of Cl_2 in the flow reactor (typically 3 mTorr) was estimated from the small change in the total pressure that was observed upon addition of the Cl_2-in-N_2 mixtures. The [alkane] was varied from $\sim 3 \times 10^{13}$ cm^{-3} to 10^{15} cm^{-3} and there were no significant changes in the experimental results indicating that the initiating reaction of Cl + alkane was limited by the Cl atom concentration and that the reaction of RO_2 with Cl atoms did not occur at a significant rate.

2.2. Sampling and detection

A schematic drawing of the flow reactor and PTr-MS is shown in Fig. 1. The outlet of the flow reactor was connected to the drift region of a PTr-MS by a large glass port (5 cm i.d..) This port acted both as a sampling port and as a drift region where the reagent ions $H^+(H_2O)_n$ reacted with trace species in the reactor effluent. Two glass ports with two different ion drift region configurations have been used in this study: one of 5 cm i.d. and ion path length of 2.7 cm used previously for the detection of ammonia at atmospheric pressure [24], and one specially constructed for this study of a path length of 12.7 cm (Fig. 2). The ion source for both is a small cylindrical volume ($\sim$1.2 cm $\times$ 1.2 cm diameter) the inner surface of which is covered by a strip of radioactive material (0.6 mCi ^{241}Am.) Each version of the IDR could be used either at the pressure of the flow reactor (several hundred Torr), or at about 10 Torr by placing a plate holding a small disk (50 μm thick) with a 300-μm hole at the top of the glass port. The resulting product ions were detected, along with reagent ions, in a differentially pumped mass spectrometer [25]. Generally, 20–50 sccm of N_2 containing trace amounts of H_2O ($\sim$0.03%) was flowed through the source. The water was taken from the vapor over slightly acidified water

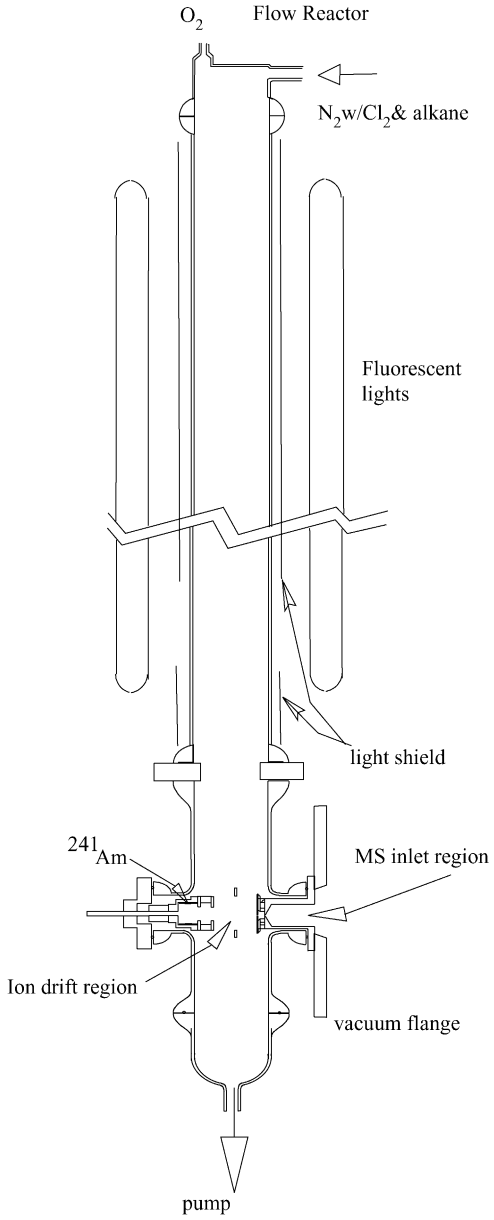

Fig. 1. Schematic drawing of the flow reactor with UV lights, ionization region and mass spectrometer.

($\sim$1 wt.% H_2SO_4) via an atmospheric pressure diffusion tube apparatus. The ion drift time (t_d) ranged between 1×10^{-4} and 1×10^{-3} s depending on electric field (200–1000 V/cm), total pressure (10–600 Torr), and drift region length.

2.3. Ion-molecule proton transfer reaction

Ion-molecule reactions such as

$$R + H_3O^+ \cdot (H_2O)_n \rightarrow RH^+ \cdot (H_2O)_m + (n-m+1)H_2O \quad (4)$$

are typically fast for $n = 0$ if the proton affinity of the neutral reactant is greater than that of H_2O. For higher n, the efficiency of the reaction might decrease owing to differences in the energetics of the various clusters in the reaction (note that values for m for a particular reaction are generally not known for $n > 0$.) In a typical IDR utilizing $H_3O^+ \cdot (H_2O)_n$ reactant ions, the ions have high drift speeds and attain a high temperature due to collisions with neutral gases; ions with n = 0 and 1 can be made to be the most abundant for IDR total pressures less than $\sim$10 Torr. However, if the IDR is operated at relatively high pressures (100 Torr or greater), high ion drift velocities cannot be maintained due to the unrealizable electric field strengths that would be necessary, and the ions are characterized by distributions where $n = 3$–5 are the most abundant, even at very low [H_2O]. Note that the typical distribution of product ions we observed had values for m of 0, 1, and 2 with the most abundant usually being $m = 1$.

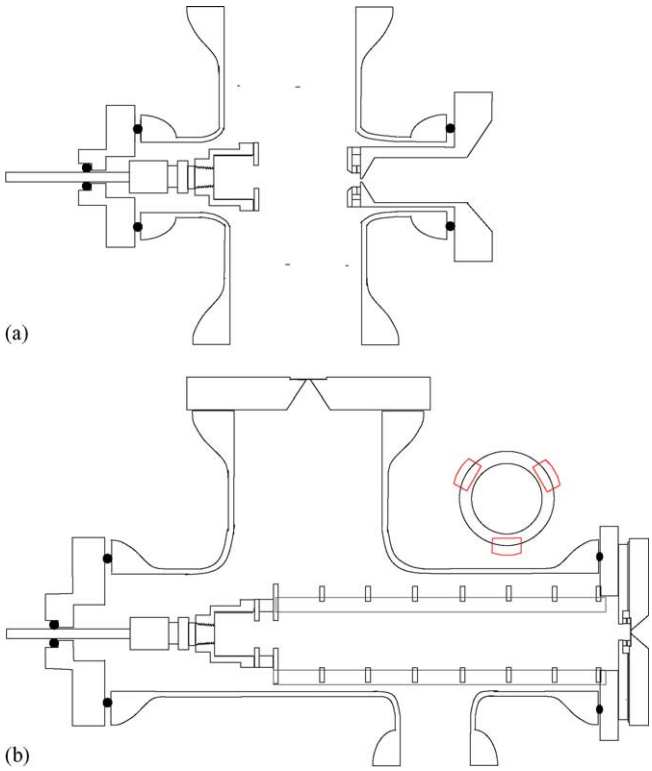

Fig. 2. (a) Ion drift region configuration used for the majority of the measurements. (b) Alternate drift region used for some studies, generally at total pressures in this region of $\sim$10 Torr.

In general, alkanes do not react with any water proton clusters thus their presence at the large concentrations here does not disrupt the abundance of reagent ions. In general, if a species contains a carbonyl or alcohol functionality, it can be ionized rapidly for a wide range of n [1,26,27], although special cases may exist. It has been shown that small RO_2 species can be ionized according to Eq. (4) for n as high as four although the ionization efficiency is not known [17–20]. Furthermore, the detection efficiency for products such as the alkyl nitrates as well as other oxidation products (e.g., the multifunctional species) are not known.

For a distinct ion-molecule reaction, the concentration of the neutral species R is related to the ion signals via

$$[\mathrm{R}] = \frac{1}{k_n t_\mathrm{d}} ln\left(1 + \frac{S_\mathrm{X}}{S_0}\right) \quad (5)$$

where k_n is the ion-molecule reaction rate coefficient, t_d is the ion drift time, and S_0 and S_X are the observed signals due to the ionizing agent and species X, respectively. This equation is based on the assumption that there are no ion mass discrimination effects (sampling, transmission, detection) within the system. Additional complications arise in the use of Eq. (5) if ion-molecule reactions such as Eq. (4) are employed and a range of ionizing agents (n) are present (e.g., Eq. (5) then may not be the solution to the differential equations that govern the ion concentrations.) However, if [R] is low enough such that S_X/S_0 is small, Eq. (5) can be approximated as

$$[\mathrm{R}] \cong \frac{1}{k_n t_\mathrm{d}} \frac{S_\mathrm{X}}{S_0} \quad (6)$$

where now $S_\mathrm{X} = \sum S_{\mathrm{RH}^+\cdot(\mathrm{H_2O})_m}$ and $S_0 = \sum S_{\mathrm{H_3O}^+\cdot(\mathrm{H_2O})_n}$. This approach assumes that k_n is not significantly dependent on n.

If [R] is known in an experiment, the sensitivity of the instrument *Sens* can be calculated from the observed product ion signals,

$$Sens\,(\mathrm{Hz\,cm^3\,molecule^{-1}}) = \frac{S_\mathrm{X}}{[\mathrm{R}]} \quad (7)$$

This sensitivity can be compared to a theoretical sensitivity TS from Eq. (6)

$$\mathrm{TS} \cong \frac{S_\mathrm{X}}{[\mathrm{R}]} = k_n t_\mathrm{d} S_0 \quad (8)$$

By comparing Eqs. (7) and (8), the proton transfer rate coefficient k_n can be estimated. As the measured sensitivity Eq. (7) is a conglomeration of water ligands, the k_n will represent a weighted average over n, with the weight depending on the abundance of the nth cluster in $\mathrm{H_3O^+\cdot(H_2O)}_n$. This distribution over n is not easily measured but can be calculated with the thermodynamics of Lau et al. [28] along with $[\mathrm{H_2O}]$ and the effective ion temperature [25,29].

2.4. Determination of sensitivities and yields

2.4.1. Peroxyl radical detection sensitivities

A known amount of NO was titrated with $\mathrm{RO_2}$ to provide an estimate of the $[\mathrm{RO_2}]$ concentration, and from Eq. (8) a value for the ion-molecule rate coefficient was obtained. The experiments were performed with the top 20 cm of the flow reactor illuminated with UV light allowing for reaction times of ∼15 s. The change in $[\mathrm{RO_2}]$ was similar to the amount of [NO] that was added with small corrections for wall loss and secondary reactions, e.g., for ethane oxidation,

$$\mathrm{CH_3CH_2O_2 + NO \rightarrow CH_3CH_2O + NO_2} \quad (9)$$

$$\mathrm{CH_3CH_2O + O_2 \rightarrow CH_3CHO + HO_2} \quad (10)$$

$$\mathrm{HO_2 + NO \rightarrow OH + NO_2} \quad (11)$$

$$\mathrm{OH + C_2H_6(+O_2) \rightarrow CH_3CH_2O_2} \quad (12)$$

$$\mathrm{CH_3CH_2O_2 + HO_2 \rightarrow CH_3CH_2OOH + O_2} \quad (13)$$

$$\mathrm{RO_2 + RO_2 \rightarrow products} \quad (14)$$

The effects of reactions (10) to (14), wall loss, and formation of alkyl nitrates were determined using box model simulations (using the Acuchem software package [30]) of the reactor conditions. Note that the change in $[RO_2]$ that we observe is not a direct measure of the $[\mathrm{RO_2}]$ that interacts with the added NO if wall loss or self-reaction are significant loss processes. In effect, there is a decrease in the amount of $\mathrm{RO_2}$ that is lost to self-reaction or the wall when NO is present. These losses were significant in the $\mathrm{CH_3O_2}$ and $\mathrm{C_6H_{11}O_2}$ experiments, and, for typical conditions, the model indicates that the observed $\Delta[\mathrm{RO_2}]$ will be 20–40% less than the added [NO]. The model predicted deviation of the observed $\Delta[\mathrm{RO_2}]$ from the added [NO] ($\Delta[\mathrm{RO_2}]/[\mathrm{NO}]$ was typically −0.75) for the cyclohexyl peroxy radical experiments was mainly due to the wall loss for this species. However, for the small peroxyls, ring opening does not occur (see below), reaction (10) occurs to a greater extent, $[\mathrm{HO_2}]$ increases, and reactions (11) and (13) are important. For ethyl peroxy radicals, where wall loss and self-reaction were not important, the model results in a $|\Delta[\mathrm{RO_2}]|$ that is approximately 150 and 125% of [NO] for $[\mathrm{NO}] = 10^{10}$ and $2 \times 10^{10}\,\mathrm{cm^{-3}}$, respectively. The dependence of $\Delta[\mathrm{RO_2}]$ on [NO] reflects the competition of reactions (11) and (13) for $\mathrm{HO_2}$ radicals. For the $\mathrm{CH_3O_2}$–NO titration experiments, self-reaction (14) is very fast and can dominate the loss for $\mathrm{CH_3O_2}$. The model predicts that the observed $|\Delta[\mathrm{CH_3O_2}]|$ is about 70% of the added [NO] for $[\mathrm{CH_3O_2}] = 2 \times 10^{10}\,\mathrm{cm^{-3}}$ to $3 \times 10^{10}\,\mathrm{cm^{-3}}$ and $[\mathrm{NO}] = 1 \times 10^{10}\,\mathrm{cm^{-3}}$. For the present experimental conditions, the effect on $\Delta[\mathrm{CH_3O_2}]$ of the self-reaction (14) is larger than that of reactions (11) and (13).

The wall loss rate coefficient for the radicals was estimated by generating $\mathrm{RO_2}$ radicals at the bottom of the flow reactor and comparing the $\mathrm{RO_2}$ signals to the $\mathrm{RO_2}$ signals obtained when radicals were formed at the top of the flow reactor. These two regions were set to have the same amount of area of the flow reactor illuminated and it was assumed that a similar number of radicals were generated in each case. These measurements for cyclohexyl peroxyl resulted in a loss of ∼20% in which results a first-order wall loss rate coefficient of $\sim 0.02\,\mathrm{s^{-1}}$. The wall loss rate coefficient for ethyl peroxyl was essentially non-existent ($\leq 0.01\,\mathrm{s^{-1}}$) however, the self-reaction resulted in losses of 5–20% depending upon initial amount of $\mathrm{RO_2}$. For methylperoxy, observed losses were large (up to 60%) and could be attributed to the self-reaction thus a wall reaction was not included. The level of added NO was chosen to be about equal to 1/2 of the initial amount of $\mathrm{RO_2}$; they were varied over the range $1–3 \times 10^{10}$ molecules $\mathrm{cm^{-3}}$ and $2–10 \times 10^{10}$ molecules $\mathrm{cm^{-3}}$, respectively.

Table 1
Rates of key reactions used to model the chemistry following reaction of cyclohexyl- and cyclopentyl-peroxy radicals with excess NO

Reaction[a]	Rate coefficient[b] (cyclohexane)	References	Rate coefficient[b] (cyclopentane)	References
1	5.9×10^{-12}	[37]	9.6×10^{-12}	[43]
1n	1.1×10^{-12}	[8,35,37,38]	1.4×10^{-12}	[42][c]
2ro	7×10^{4} s^{-1}	[8,31,32,35,37,38]	$>1 \times 10^{6}$ s^{-1}	[38]
2a	1×10^{-14}	[39–42][c]	1×10^{-14}	[39–42][c]
3	7.4×10^{-12}	[40,42][c]	7.6×10^{-12}	[40,42]
3n	0.6×10^{-12}	[42][c]	4×10^{-13}	[42][c]
4a	1×10^{-14}	[39–42][c]	1×10^{-14}	[39–42][c]
4i	2×10^{6} s^{-1}	[39][c]	2×10^{6} s^{-1}	[39][c]
5	6.6×10^{-12}	[40,42][c]	7×10^{-12}	[40,42][c]
5n	1.4×10^{-12}	[42][c]	1×10^{-12}	[42][c]
6i	7×10^{6} s^{-1}	[39][c]	7×10^{6} s^{-1}	[39][c]
6d	$\approx 10^{5}$ s^{-1}	[39,41][c]	$>1 \times 10^{7}$ s^{-1}	[41][c]
7a′	1.0×10^{-11}	[22][c]	n/a	

[a] See Figs. 5 and 7 for identity of reactions.
[b] Rate coefficients in units of cm^3 molecule^{-1} s^{-1} unless otherwise noted.
[c] Rate coefficients are estimates based on relevant data given in the cited reviews.

2.4.2. Product studies

End products were investigated for the cyclohexyl peroxy and cyclopentyl peroxy + NO reactions by adding [NO] in large excess over [RO_2]: typically 2×10^{12} and 1×10^{11} cm^{-3}, respectively. Average flow reactor residence time was ∼3 s. Partial pressure of O_2 was generally 45 Torr out of ∼100 Torr total, although this was varied at times (from 1 to 80 Torr). Box model simulations of the reaction conditions were carried out, again using Acuchem, and the expected yields of the products from the box model were used to evaluate the sensitivities of the instrument towards the various product species. Rate coefficient data used in the model were from Sander and co-workers [22], from previous studies of cyclopentane and cyclohexane chemistry [8,31–38] or were estimated using reviews and structure-reactivity relationships available in the literature [39–42]. Table 1 presents a summary of the rate coefficients used in the box model whose values have the most significance for the reported yields.

3. Results

3.1. The reaction of $H_3O^+ \cdot (H_2O)_n$ with RO_2

Typical experiments are depicted in Fig. 3 where the signals due to the cyclohexyl, ethyl, and methyl peroxy radicals are shown as a function of time (additions of NO are indicated in the figures.) In Fig. 3a, the $\Delta[C_6H_{11}O_2]$ at the level of the detector due to the addition of [NO] = 1.2×10^{10} cm^{-3} is calculated to be 0.9×10^{10} cm^{-3}. Using (6) above, the observed reagent ion signal $S_0 = 2.7 \times 10^5$ Hz, and the t_d of 2.8×10^{-4} s, k_n is equal to 1.8×10^{-9} cm^3 molecule^{-1} s^{-1}. This type of experiment was repeated for the methyl and ethyl peroxy radicals and the observed detection sensitivities resulted in k_n of ∼0.8 and 0.55×10^{-9} cm^3 molecule^{-1} s^{-1}, respectively. These values are listed in Table 2 along with other relevant experimental details and have estimated uncertainties of +100/−50% primarily due to uncertainties in the method for determining [RO_2].

We found that small amounts of water vapor significantly decreased the sensitivity of the instrument for detection of RO_2. This is shown in Fig. 4 where the signals for CH_3O_2, $C_2H_5O_2$ and $C_6H_{11}O_2$ are plotted versus the partial pressure of H_2O, pH_2O. Even at low water pressures, $\sim 10^{-5}$ atm, a significant decrease in the sensitivity of the instrument was noted, especially for the small alkyl peroxy radicals. The effect was larger for methyl peroxy than for ethyl peroxy while that for cyclohexyl peroxy was modest. Two sets of data for the ethyl peroxy radical are shown for two different electric field strengths. Based on these data where a lower effect of water was observed at a higher field strength, a change in the distribution of the proton-water clusters (dominant ions at 73 and 37 amu for the two different experiments) could be partly responsible for this effect. However, the ion distribu-

Table 2
Rate coefficients for $RO_2 + H_3O^+ \cdot (H_2O)_n$

Peroxy radical	k_n (cm^3 s^{-1})	Range of n[a]	E/N[b]	Product ion distribution, $RO_2 \cdot H^+ \cdot (H_2O)_m$ (%)[c]
$C_6H_{11}O_2$	1.8×10^{-9}	17%, $n=2$; 82%, $n=3$	18	35, 62, 3, ∼0.1
$CH_3CH_2O_2$	0.8×10^{-9}	17%, $n=2$; 82%, $n=3$	18	8, 59, 32, 1
CH_3O_2	0.56×10^{-9}	67%, $n=2$; 33%, $n=3$	34	4, 48, 42, 6

$pH_2O \leq 2 \times 10^{-6}$ atm. Estimated uncertainty is +100/−50%.
[a] Equilibrium distributions assuming $pH_2O = 2 \times 10^{-6}$ atm, see text.
[b] Electric field E divided by total number density N (N in units of 10^{17} molecule cm^{-3}), 10^{17} V cm^{-1} cm^3 molecule^{-1}.
[c] $m=0$, $m=1$, $m=2$, etc.

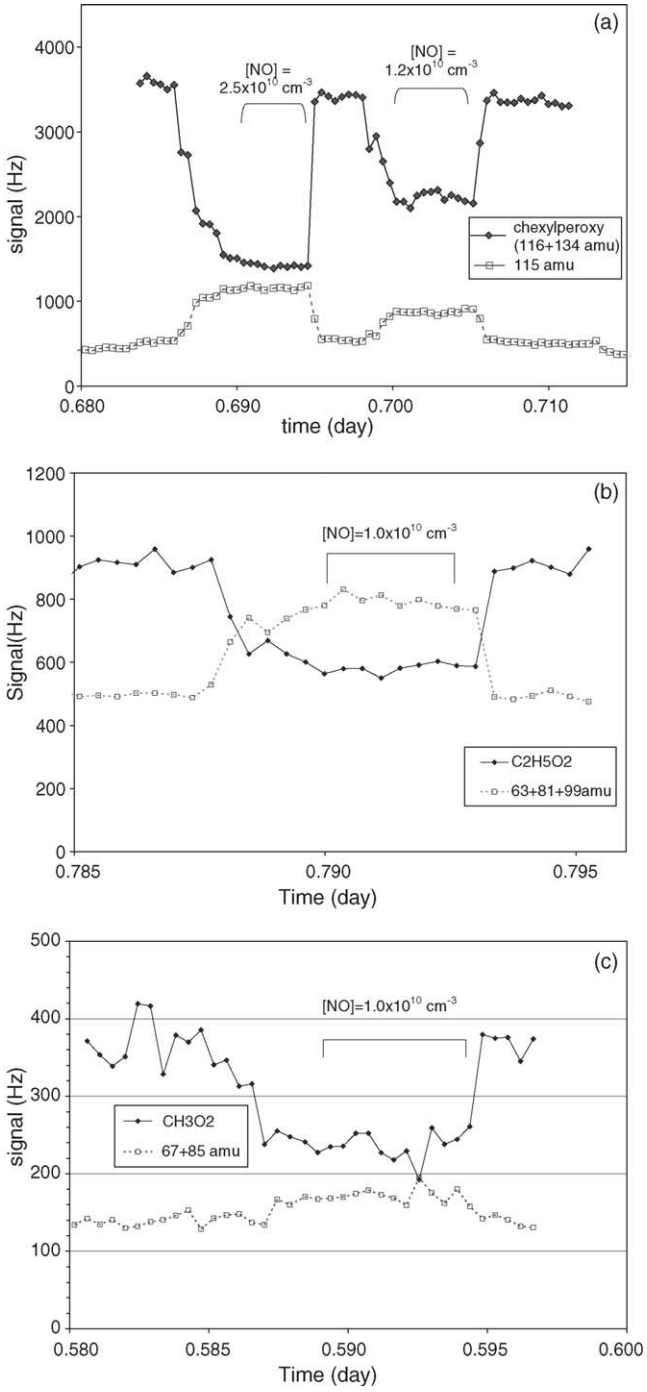

Fig. 3. Signals due to the (a) cyclohexyl, (b) ethyl, and (c) methyl peroxy radicals. Additions of NO are indicated in the figures. (a) Sum of signals at 116 and 134 amu due to the cyclohexyl peroxy radical (S_0 = 275 kHz, 18 Td, 91 Torr total pressure, initial RO_2 at the level of the detector, $[C_6H_{11}O_2]_0$, was approximately 3.4×10^{10} cm^{-3}). Signal at 115 amu due to hexanedial and possible a nitrate species is also shown. (b) Sum of signals at 62, 80, and 98 amu due to the ethyl peroxy radical (S_0 = 100 kHz, 18 Td, 91 Torr total pressure, average $[C_2H_5O_2]_0 \sim 4.1 \times 10^{10}$ cm^{-3}). Sum of signals at 63, 81, and 99 amu due to acetaldehyde and ethyl hydrogen peroxide are also shown. (c) Sum of signals at 48, 66, 84, 102 amu due to the methyl peroxy radical (S_0 = 220 kHz, 34 Td, 90 Torr total pressure, detector $[CH_3O_2] = 2.2 \times 10^{10}$ cm^{-3}). Sum of signals at 67 and 85 amu due to formaldehyde and methyl hydrogen peroxide are also shown.

tions [28] for the weak and strong fields are dominated by 73 and 37 amu, respectively, over the entire range of pH_2O investigated which suggests a more complicated explanation. The observed exponential decrease in sensitivity with added water vapor for the ethyl peroxy radical would not be consistent with the establishment of an ion-molecule equilibrium (i.e., occurrence of a thermal and reversible reaction.) Note that an ion-molecule equilibrium affecting the detection of the CH_3O_2 radical is not ruled out here as there is not enough data to ascertain the functional relationship. It is possible that a reaction of the 'heated' (due to the drift field) $RO_2{\cdot}H^+(H_2O)_m$ species occurs upon collision with another water molecule that results in the formation of a water proton cluster and the regeneration of the RO_2 species. A definitive conclusion on the water effect awaits further experimental work.

3.2. End product analysis

The chemistry occurring upon addition of NO to the cyclohexyl and cyclopentyl peroxy radicals was investigated. A typical experiment proceeded as follows. First, peroxy radicals were generated as before (without NO present) from the reaction of Cl with the parent alkane in the presence of O_2. Typical radical levels, as determined by PTr-MS, were 1×10^{11} cm^{-3} to 2×10^{11} cm^{-3}. Then, excess NO, about 2×10^{12} cm^{-3} to 3×10^{12} cm^{-3}, was added to the flow reactor. With NO present, the peroxy radicals are rapidly converted to the corresponding alkoxy radical. Under the conditions of our experiments, ring-opening is the major fate of the cyclo-alkoxy radicals (e.g., [38]), and subsequent chemistry leads to the production of a complex suite of multi-functional species (see below). HO_2 is generated in large yields in this chemistry; its reaction with NO generates OH, which in turn regenerates the parent cyclic peroxy radical. Simulations of typical reaction conditions indicated a chain length of ≈2.5, i.e., 1.5 additional cyclohexyl or cyclopentyl peroxy radicals are formed for each radical initially formed in the reaction of with Cl with the parent cycloalkane. Box model simulations also showed that radical termination was predominantly via the formation of organic nitrates:

$$RO_2 + NO + M \rightarrow RONO_2 + M \quad (15)$$

where RO_2 indicates any organic peroxy radical. Essentially all radicals are converted to nitrates in 0.5 s, much shorter than the shortest flow reactor residence times (∼3 s) that were used.

3.2.1. Cyclohexane

The chemistry likely to occur following reaction of cyclohexyl peroxy radicals with NO, as outlined in detail by Aschmann et al., [8] is presented in Fig. 5. Shown in Fig. 6 is a difference mass spectrum, obtained by subtracting two spectra: one acquired in the presence and one in the absence of NO. For this particular experiment, the total pressure in the flow reactor was 100 Torr, the O_2 partial pressure was 45 Torr, the initial $[RO_2]$ and [NO] were 1.0×10^{11} and 2.6×10^{12} cm^{-3},

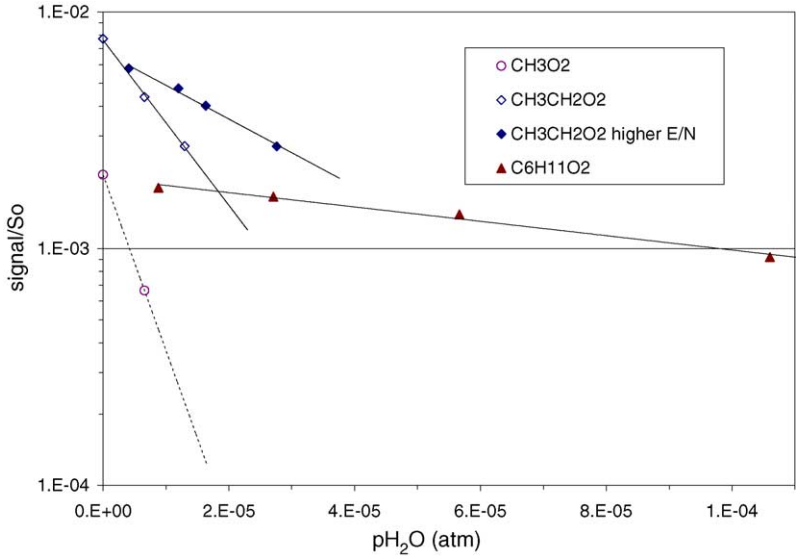

Fig. 4. Detection of methyl, ethyl, and cyclohexyl peroxy radicals in the presence of added H_2O. Total pressure was 91 Torr and electric field strength (E/N) = 20 Td (methyl- and ethyl-peroxyl data points, using IDR of Fig. 2a) 10 Torr and E/N = 90 Td (solid ethylperoxy data), and 10 Torr and 66 Td for the cyclohexyl peroxy data (the latter two sets of data were taken using the IDR of Fig. 2b). The amount of H_2O entering the drift region from the ion source was not included in this data. If it were to become fully mixed with the flow from the flow reactor, which is unlikely in the short residence time, it would amount to $pH_2O = \sim 2 \times 10^{-6}$ atm.

respectively. Compounds detected in the product spectrum are identified with asterisks in Fig. 5. Table 3 presents signal-derived yields for these products, assuming that the sensitivities for all products were equal to that of the cyclohexyl peroxy radical, and assuming a chain length of 2.3 ± 0.5 as determined by box model simulations.

The largest product ion signal is at mass 113 and, we believe, the associated mass peaks at 85, 103, 71 and 89. The 113, 85, and 71 amu ions have been shown to be due to fragmentation of the 131 amu ion [8]; the ion formed in the reaction of water proton clusters with the 3-hydroxy-hexanedial, $HC(O)CH_2CH(OH)CH_2CH_2CHO$. Therefore, the majority of the signal at these masses (plus 103 and 89 which are probably water ligands on 85 and 71 amu, respectively) is likely due to this species. As was observed in the Aschmann et al. [8] study, we observed a small signal at 131 amu, which is consistent with this interpretation. The total ion signal that corresponds to this species is about 0.9 times the initial RO_2 signals (116 + 134 + 152 + 170) resulting in a signal-derived yield of 0.9/2.3 = 0.39. This is in rough accord with the box model prediction, which states that this species should have a yield of 0.48. The difference could be due in part to a lower sensitivity of the instrument (i.e., slower ion-molecule rate coefficient) towards the 3-hydroxy-hexanedial than towards the RO_2 species.

The next largest product ion signals at 99 and 117 amu are primarily due to cyclohexanone, the H^+·cyclohexanone and water ligand ions, respectively. Published data [8,38] indicate that cyclohexoxy radicals should react with O_2 to give HO_2 and cyclohexanone about 15% of the time at 45 Torr O_2. This can be compared with the yield we obtain from the signal ratios ($\Delta S_{cyclohexanone}/2.3\Delta S_{RO2}$) which was about 28%. The instrument might therefore be more sensitive towards cyclohexanone than the RO_2 radical, which is consistent with the general expectation that reactions of ketones with water proton clusters are fast. In experiments where O_2 was varied (2–80 Torr), we observed a near linear dependence of the cyclohexanone yield upon partial pressure of O_2, which is in accord with the knowledge of this oxidation step [8,38]. There was a non-zero intercept for these data possibly indicating the contribution of a wall reaction to the observed cyclohexanone. In addition, another species, perhaps a nitrate, may contribute to the signal at 99 amu (see Section 3.2.3)

The nitrate species produced in the reaction of NO with RO_2 radicals were also detected. These are evident in Fig. 6 (note the scale change, parent·H^+ underlined) at masses 146 + 164 + 182, cyclohexylnitrate; 162 + 180 + 198, 6-nitrooxy-hexanal; and 160 + 178 + 196, 3-nitrooxy-6-hydroxy-hexanal. The signal levels observed for the cyclohexyl nitrate amounted to about a 3% yield which is considerably smaller than the expected [8,37,38] yield of 15%. Apparently, the ionization efficiency by water proton clusters of the cyclohexyl nitrate species is very low compared to that for RO_2. This is consistent with the observed very weak signal at this mass reported by Aschmann et al. [8] In addition, it is possible that fragmentation of the 146 amu ion occurred (see Section 3.2.3) resulting in a weak signal at masses 146 + 164 + 182. The species at 162 amu (+hydrates) was also observed by Aschmann et al. and was identified as 6-nitrooxy-hexanal, $O_2NOCH_2CH_2CH_2CH_2CH_2CHO$. The comparison with the box model results for this species (3.6% observed from signal ratio, 5% yield in the box model) suggests better detection efficiency at M·H^+ plus water ligands than for the simple alkyl nitrate.

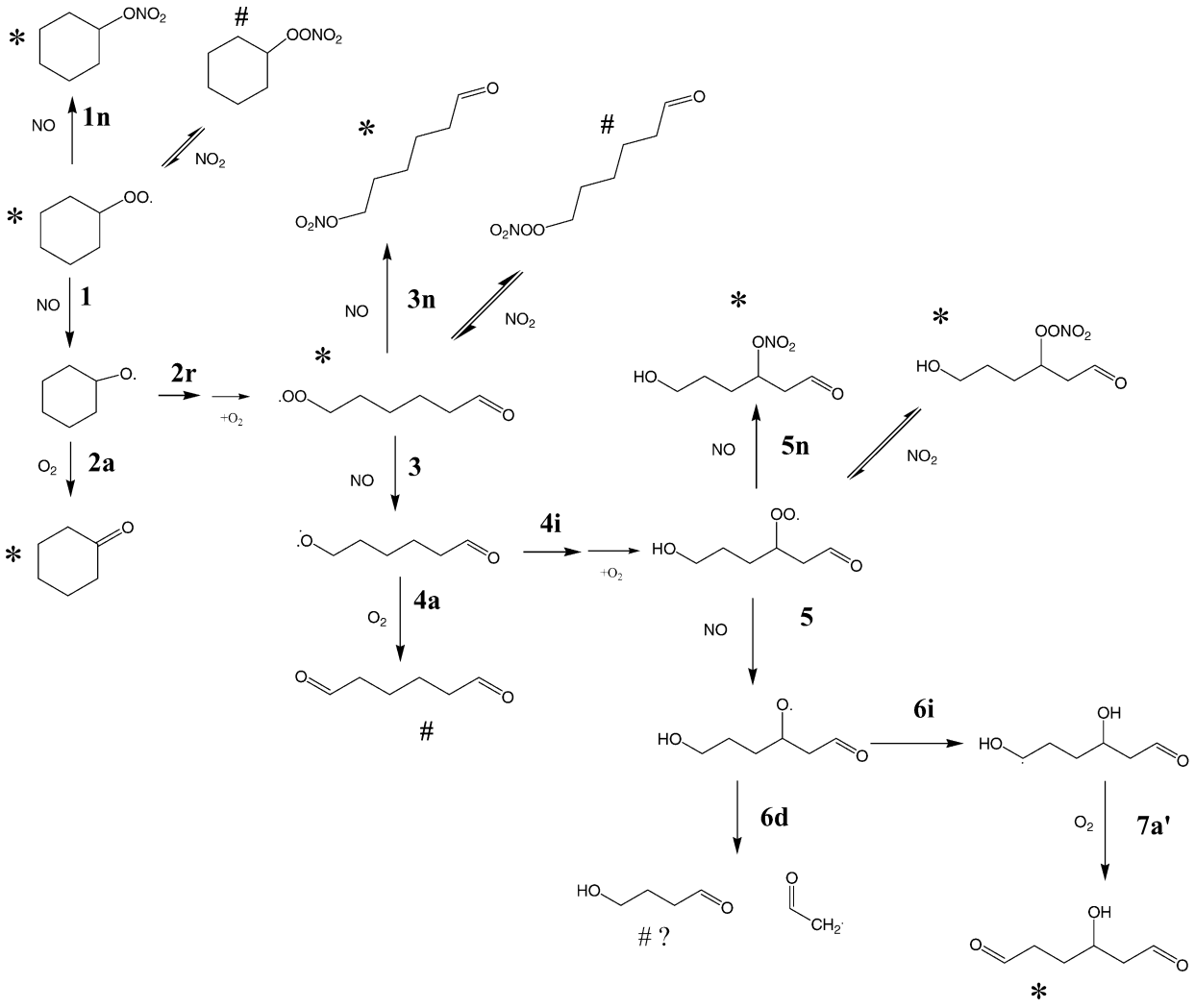

Fig. 5. Major reactions expected from the reaction of cyclohexyl peroxy radicals with NO. The symbol (*) indicates a species that was detected in this study, and (#) indicates a minor species whose product ion may overlap with the more abundant species.

Aschmann et al. [8] did not observe the 3-nitrooxy-6-hydroxy-hexanal species ($M{\cdot}H^+$ at 178 amu) that is formed in the reaction of the intermediate radical $HOCH_2CH_2CH_2C(OO^{\bullet})HCH_2CHO$ with NO (reaction 5n in Fig. 5). Perhaps their ionization conditions did not allow for the initial proton transfer or the ion sampling from atmospheric pressure led to fragmentation of $M{\cdot}H^+$ for the products. The fragment ions may not have been noticeable if they fell on peaks with high count rates. For example, the 178 amu could lose an HNO_3 molecule leaving an ion at 115 amu. In fact, we believe this could have happened in our experimental apparatus. Predicted versus observed signals for 3-nitrooxy-6-hydroxy-hexanal at 178 amu (11% versus ~3%) indicates that the detection sensitivity for this nitrate species is less than that for $C_6H_{11}O_2$ and cyclohexanone. However, the comparison might be improved if we attribute some of the signal at 115 amu to this species. The signal at 115 amu indicates a 3.4% yield due to the dialdehyde (assuming a sensitivity similar to that for RO_2), much higher than the predicted yield for this species, ~0.5%. Thus it is reasonable to postulate that the 178 amu ion can lose an HNO_3 molecule and appear at 115 amu and the predicted versus observed product ion yield comparison improves (11% versus 6%.) It does appear that the substituted nitrates are somewhat more easily ionized by water proton clusters than are the simple alkyl nitrates. Finally, it is important to note that three peroxylnitrate species, of $M{\cdot}H^+$ masses = 162, 178, and 194 amu are predicted to be have yields in the 0.7 to 1% range. The signals observed at 194 and 212 amu result in a yield of about 0.8% and can be assigned to the protonated $HOCH_2CH_2CH_2CH(OONO_2)CH_2CHO$ (3-nitroperoxy-6-hydroxy-hexanal) species and its hydrate, indicating that the detection of the other peroxynitrates is likely. Thus the 162 and 178 amu ($M{\cdot}H^+$) peroxylnitrate species probably contribute to the signals we attributed to the nitrate species in the preceding discussion.

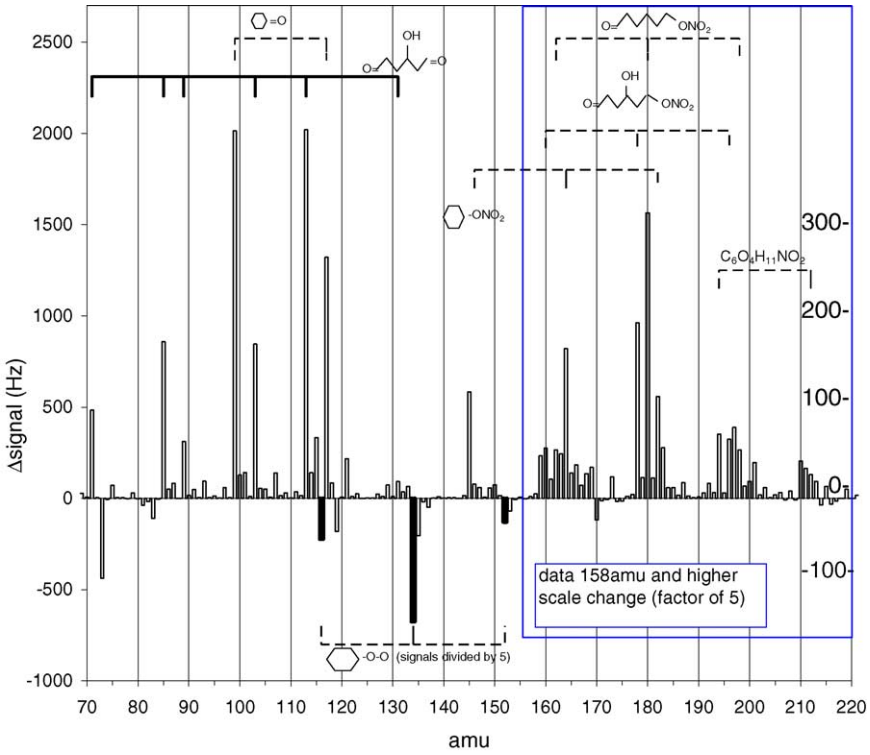

Fig. 6. Difference between mass spectrum taken with and without NO present for the Cl_2/cyclohexane/O_2/N_2 system. Total pressure was 93 Torr for the flow reactor and for the IDR (the IDR was that shown in Fig. 2a and the O_2 partial pressure was 45 Torr. The electric field was ∼700 V/cm resulting in an *E*/*N* of 18 Td (1 V/cm per 10^{17} cm^{-3}).

Table 3
Products observed in oxidation of cyclohexane

Reaction[a]	Product	Model yield (%)	Exp. yield (%)[b]	$M{\cdot}H^+$ (water ligands, fragments) amu	Comment on ion chemistry[c]
7a′	3-Hydroxy-hexane-dial	48	39	131 (71, 85, 89, 103, 113, 149)	89 amu ion would obscure the detection of any product 6d
2a	Cyclohexanone	15	28	99 (117, 135)	Minor contribution from breakup of ion due to 146 and 162 amu species
1n	Cyclohexyl nitrate	15	3.2	146 (164, 182, 200)	$M{\cdot}H^+ \rightarrow$ 99 amu ion + HONO
–	Unidentified	–	5	145	Yield varies, no clear dependence on experimental conditions
4a	Hexane dialdehyde	0.5	3.4	115 (133)	Contribution from breakup of ion due to 162 and 178 amu species
5n	6-Hydroxy-3-nitrooxy-hexanal	11	2.6	178 (160, 196)	$M{\cdot}H^+ \rightarrow$ 115/131 amu ion + HNO_3/HONO
3n	6-Nitrooxy-hexanal	5	3.6	162 (180, 198)	$M{\cdot}H^+ \rightarrow$ 99/115 amu ion + HNO_3/HONO
–	Cyclohexanol	<0.01	∼1.2	101	(i) $146{\cdot}H_2O$ ion → 101 amu ion + HNO_3. (ii) Cyclohexanol product of wall reaction? Yet 119 amu ion, $M{\cdot}H^+{\cdot}H_2O$, decreased upon addition of NO.
	6-Hydroxy-3-nitrooxy-hexanal	0.9	∼0.8	194 (212)	

[a] Reaction number depicted in Fig. 5.
[b] Assuming identical sensitivities for the products as was obtained for the peroxy radical and using a modeled chain length of 2.3. Signal obtained from the difference between signals with and without NO added. Thus the effects of wall loss and self-reaction, that could depend upon the presence of NO, were neglected for this calculation. The product ions used are shown in the next column.
[c] Potential water ligands are not considered here when listing the ion mass.

In a series of experiments at higher *E*/*N* (42–83 Td; using the IDR of Fig. 2b and a low pressure in the IDR), we observed a marked decrease in the detection of the nitrate species as *E*/*N* was increased. For the detection of 6-nitrooxy-hexanal, for example, the signal at 162 + 180 amu was 7, 3, and <1% of Δ(116 + 134 + 152 amu) at 42, 63, and 84 Td respectively.

There are a number of small mass peaks (each <1% of the total product ions) that appear in the mass spectrum in Fig. 6. There are two sets of ions in Fig. 6 that we can tentatively assign to species. A C6 species such as a hydroxy-dicarbonyl-nitrate or a peroxylnitrate-dicarbonyl (both with $M{\cdot}H^+ = 192$ amu) could give the ions observed at 192 and 210 (+ H_2O) amu. Finally, it appears that there are detectable signals at 132, 150, and 168 amu. These might be due to the peroxy radical formed following ring opening: $HC(O)(CH_2)_4CH_2OO$ ($M{\cdot}H^+ = 132$ amu) and its hydrates. The sum of these peaks is ∼2% of the initial cyclohexyl peroxy radical signals which is in rough accord with the box model prediction of ∼1%.

There was a fairly large signal (∼6% of the total product ion signal) that appears at 145 amu in the data shown in Fig. 6. This species is difficult to assign and could be due to an impurity in the system. Later experiments show smaller signals at 145 amu (∼2% of the total product signal.) It is possible that the species at 192 amu could contribute to the signal here if it were to lose an HONO molecule (the small peak at 129 amu could be due to loss of HNO_3 from 192 amu). The losses of HONO and/or HNO_3 that we have postulated have in common that the initial nitrate species contains an OH group. It is also known that the products of proton transfer reactions with peroxyacyl nitrates can lose HNO_3 molecules [44].

3.2.2. Cyclopentane

The chemistry expected to occur following reaction of NO with cyclopentyl peroxy radicals is outlined in Fig. 7 [8,31–34,38]. These previous studies have shown that ring-opening is the dominant, if not exclusive, fate of the cyclopentoxy radical. However, the ring-opening products have not been extensively investigated: the products that have so far been identified are CO, CO_2 and formic acid [38]. Compounds identified in the PTr-MS product spectra are highlighted in Fig. 7 with asterisks and are also listed in Table 4. Also given in Table 4 are the signal-derived yields for these species (again assuming equal sensitivity for each of the products as for the peroxy radical and assuming a chain length of 2.5 ± 0.5), and the yields obtained from box model simulations for comparison.

The product spectra are dominated by peaks observed due to the presence of 4-hydroxy-butanal (signals at 71, 89, and 107 amu). The signal-derived yield for this species (54%) is broadly consistent with the results from the model simulation, which suggests a 67% yield. As with the major product in the cyclohexane system, 3-hydroxy-hexanedial, the discrepancy may be the result of a lower sensitivity of the PTr-MS for the 4-hydroxy-butanal compared to the cyclopentyl peroxy radical. Although 4-hydroxy-butanal has not been previously identified from the oxidation of cyclopentane, it is the postulated co-product of the CO and CO_2 observed by Orlando et al. [38]. The fact that the 4-hydroxy-butanal is much more prominent than 2-hydroxy-pentane-dialdehyde indicates that decomposition of the $HOCH_2CH_2CH_2CH(O^{\bullet})CHO$ radical dominates over its isomerization (see **6d** in Fig. 7), a process that should occur with a rate coefficient in excess of $10^6\ s^{-1}$ [39].

Two nitrate species can be identified in the product spectra, 5-nitrooxypentanal and 5-hydroxy-2-nitrooxy-pentanal. Surprisingly, cyclopentyl nitrate is not observed even though the yield of the three nitrate species is likely to be of similar magnitude (4–12%). The lack of any signal for the cyclopentyl nitrate again points to the likelihood that the ionization efficiency of the cycloalkyl nitrates by water proton clusters is low (see Section 3.2.3 for further discussion.) The signal levels for the two substituted nitrates are also somewhat smaller than their expected yields (see Table 4), indicating limited sensitivity to these species.

Finally, peaks that can be assigned to protonated cyclopentanone (85 amu) and glutaric dialdehyde (101 amu) are present in our spectra, with signal-derived yields of about 5 and 3%, respectively. While the former compound is a likely product of the peroxy radical self-reaction, e.g.,

$$\text{c-}C_5H_9OO^{\bullet} + \text{c-}C_5H_9OO^{\bullet} \rightarrow \text{c-}C_5H_9O^{\bullet} + \text{c-}C_5H_9O^{\bullet} + O_2 \quad (16)$$

$$\text{c-}C_5H_9OO^{\bullet} + \text{c-}C_5H_9OO^{\bullet} \rightarrow \text{cyclohexanone} + \text{cyclohexanol} + O_2 \quad (17)$$

its yield should be negligible in these experiments, where the peroxy radical chemistry is dominated by their reaction with NO. It is possible that the protonated 5-nitrooxypentanal ion (148 amu) could lose an HNO_3 molecule to give an ion at 85 amu as we postulated for similar ions in the cyclohexane oxidation scheme. Furthermore, the protonated 5-hydroxy-2-nitrooxy-pentanal ion (164 amu) is even more so expected to eliminate HNO_3 (because of the hydroxy group) and this could be responsible for the ion observed at 101 amu. This is discussed further in the next section.

3.2.3. Product ion fragmentation

There are ion breakup processes in a PTr-MS that complicate the quantification of the species such as those we present here. For example, it is long known that hydroxy species easily lose a water molecule once they are protonated in a PTr-MS and the observations reported here are consistent with this scenario. It is also reported that HNO_3 can be lost from protonated nitrate containing species [44]. Previous work [20] indicates that alkyl nitrates react with water proton clusters and that the parent + proton ion ($M{\cdot}H^+$) can be preserved. Taken together with other work [16–20], it appears that the larger the alkyl 'moiety', the more efficient the proton transfer. Although quantitative ion-molecule rate coefficients for

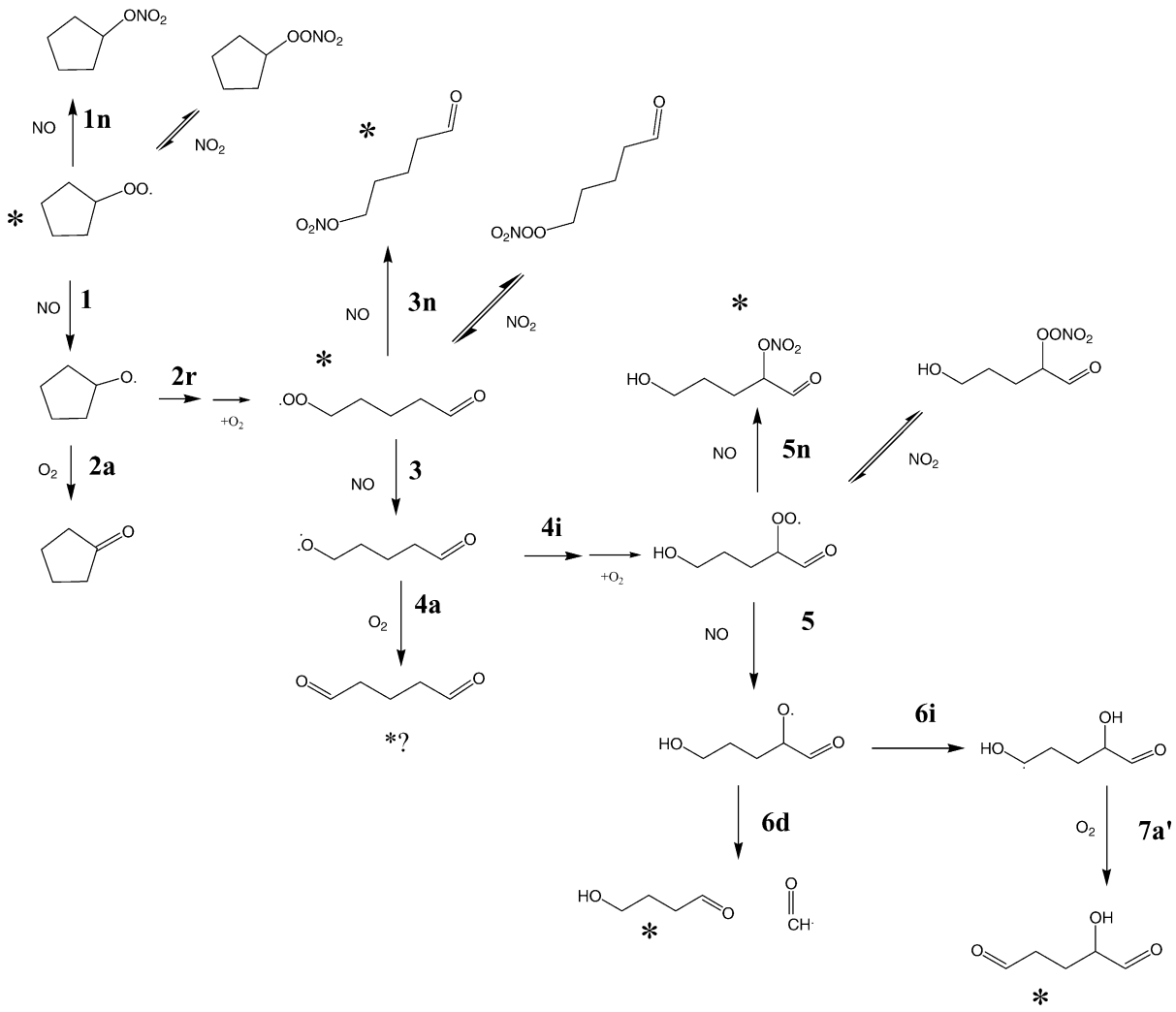

Fig. 7. Major reactions expected from the reaction of cyclopentyl peroxy radicals with NO. The symbol (*)species that were detected in this study.

the reaction of $H_3O^+(H_2O)_n$ with $RONO_2$ were not reported, it is unlikely that there is a large increase with the number of carbon atoms in the rate of protonation of an alkyl nitrate once it is as large as C5. Our limited ability to detect cyclohexylnitrate and complete inability to detect cyclopentylnitrate at $M{\cdot}H^+$ is therefore most likely due to ion breakup. We propose that the cyclic alkyl nitrates are readily protonated in the PTr-MS but that the product ion loses an HONO molecule to yield an ion that corresponds to the protonated C5 or C6 cyclo-ketone. This is most evident in the cyclopentane oxi-

Table 4
Products observed in the oxidation of cyclopentane

Reaction	Product	Model yield (%)	Exp. yield (%)[a]	$M{\cdot}H^+$ (amu)	Comment on ion chemistry
6d	4-Hydroxy-butanal	67	54	89	
7a′	2-Hydroxy-pentane-dial	4.7	4	117	
2a	Cyclopentanone	<0.01	∼5	85	Signal at 85 amu could be due to breakup of ion from 132 and 148 amu species
1n	Cyclopentyl nitrate	12	∼0	132	$M{\cdot}H^+$–HONO → 85 amu
4a	Glutaric dialdehyde	0.02	2.6	101	Signal at 101 could be due to breakup of ion from 148 and 164 amu species
5n	5-Hydroxy-2-nitrooxy-pentanal	10	3	164	$M{\cdot}H^+$–HNO_3/HNO_2 → 101/117 amu
3n	5-Nitrooxy-pentanal	4.3	3	148	$M{\cdot}H^+$–HNO_3/HNO_2 → 85/101 amu

See Table 2 for details.

[a] Relative to the initial signal due to the $C_5H_9O_2$ radical and using a modeled chain length of 2.5.

dation measurements where essentially zero cyclopentanone should be formed but a large signal was observed. This loss of HONO from simple alkyl nitrates may occur only for cyclic alkyl moieties. Evidently, more work needs to be done on the reaction of water protons + alkyl nitrates.

As discussed previously here, it is likely that the multifunctional nitrate compounds can lose HONO and/or HNO_3 molecules once they are protonated in a PTr-MS. This is bolstered by two observations: (1) a decrease in the apparent yield of the C6 nitrates with *E*/*N* discussed above and (2) signals due to ions with masses that are 47 or 63 amu less than $M{\cdot}H^+$ for a given nitrate species. Furthermore for (2), the ions could not be assigned to another species that is expected to be present in either the cyclopentane or cyclohexane oxidation processes. The detection (i.e., relative to the peroxyl radical signal and modeled yield) at $M{\cdot}H^+$ of the nitrates following ring opening was similarly deficient in the C5 and C6 systems. This indicates a similarity of ion breakup pattern with structure and this could simplify the calibration of the instrument for these types of nitrates. Finally, detection of these types of species at $M{\cdot}H^+$ may be best in a flowing afterglow type of CIMS (e.g., Elrod and co-workers. [16–20], Eberhard et al. [43], Villalta et al. [45].)

4. Summary/conclusions

We have demonstrated that PTr-MS detection of peroxyl radicals is efficient and that it will be a useful tool in kinetics studies of these types of radicals. Our detection sensitivities provide quantitive support to the hypothesis of Elrod et al. (e.g. Chow et al. [20]) that small organic peroxy radicals can react efficiently with water proton clusters up to $n = 3$. There is a deleterious effect on the sensitivities due to the presence of water vapor that could be due to shifting the water proton clusters to higher values of n or to the reaction of $RO_2{\cdot}H^+(H_2O)_m$ with water vapor.

Many product species can be identified and our results for the oxidation of cyclohexyl peroxy by NO are in accord with the results of Aschmann et al. [8]. We were able to identify a number of additional nitrate species in the mass spectrum including a peroxynitrate, $HOCH_2CH_2CH_2CH(OONO_2)CH_2CHO$. Also small signals for the secondary peroxyl $O_2CH_2CH_2CH_2CH_2CH_2CHO$ were observed.

Numerous cyclopentane oxidation products were detected for the first time. These results confirm speculation that 4-hydroxy-butanal is a dominant product of cyclopentane oxidation and they bolster confidence in the mechanisms previously presented.

Further application of this technique should result in wealth of new and confirming knowledge of the reactions of peroxyl radicals and of hydrocarbon oxidation mechanisms in general. The study of the heterogeneous chemistry of RO_2 radicals could also be accomplished using a PTr-MS type detector although it may be limited to rather low water vapor pressure compounds for small alkyl peroxy radicals.

References

[1] W. Lindinger, A. Hansel, A. Jordan, Int. J. Mass Spectrom. Ion Processes 173 (1998) 191.
[2] N.G. Adams, D. Smith, Int. J. Mass Spectrom. Ion Phys. 21 (1976) 349.
[3] T. Karl, A. Hansel, T. Mark, W. Lindinger, D. Hoffmann, Int J Mass Spectrom. 223 (2003) 527.
[4] T. Karl, P.J. Crutzen, M. Mandl, M. Staudinger, A. Guenther, A. Jordan, R. Fall, W. Lindinger, Atmos. Environ. 35 (2001) 5287.
[5] R. Fall, T. Karl, A. Jordan, W. Lindinger, Atmos. Environ. 35 (2001) 3905.
[6] C. Warneke, R. Holzinger, A. Hansel, A. Jordan, W. Lindinger, U. Poschl, J. Williams, P. Hoor, H. Fischer, P.J. Crutzen, J. Atmos. Chem. 38 (2001) 167.
[7] T. Karl, R. Fall, P.J. Crutzen, A. Jordan, W. Lindinger, Geophys. Res. Lett. 28 (2001) 507.
[8] S.M. Aschmann, A.A. Chew, J. Arey, R. Atkinson, J. Phys. Chem. 101 (1997) 8042.
[9] S.M. Aschmann, J. Arey, R. Atkinson, J. Atmos. Chem. 45 (2003) 289.
[10] S.M. Aschmann, J. Arey, R. Atkinson, J. Phys. Chem. A 105 (2001) 7598.
[11] S.M. Aschmann, E.C. Tuazon, J. Arey, R. Atkinson, J. Phys. Chem. A 107 (2003) 2247.
[12] J. Baker, S.M. Aschmann, J. Arey, R. Atkinson, Int. J. Chem. Kinet. 34 (2002) 73.
[13] R. Atkinson, E.C. Tuazon, S.M. Aschmann, Int. J. Chem. Kinet. 30 (1998) 577.
[14] S.M. Aschmann, S. Yonghui, J. Arey, R. Atkinson, Atmos. Environ. 31 (1997) 3551.
[15] A. Alvarado, E.C. Tuazon, S.M. Aschmann, J. Arey, R. Atkinson, Atmos. Environ. 33 (1999) 2893.
[16] A. Wisthaler, N.R. Jensen, R. Winterhalter, W. Lindinger, Hjorth, J. Atmos. Environ. 35 (2001) 6181.
[17] K.W. Scholtens, B.M. Messer, C.D. Cappa, M.J. Elrod, J. Phys. Chem. A. 103 (1999) 4378.
[18] M.J. Elrod, D.L. Ranschaert, N.J. Schneider, Int. J. Chem. Kinet. 33 (2001) 363.
[19] D.L. Ranschaert, N.J. Schneider, M.J. Elrod, J. Phys. Chem. A 104 (2000) 5758.
[20] J.M. Chow, A.M. Miller, M.J. Elrod, J. Phys. Chem. A 107 (2003) 3040.
[21] C.J. Howard, J. Phys. Chem. 83 (1979) 3.
[22] W.B. DeMore, S.P. Sander, D.M. Golden, R.F. Hampson, M.J. Kurylo, C.J. Howard, A. R. Ravishankara, C.E. Kolb, M.J. Molina, JPL Publication 97 –4, 1997.
[23] C.R.C. Weast (Ed.), Handbook of Chemistry and Physics, 1979.
[24] D. Hanson, E. Kosciuch, J. Phys. Chem. A 107 (2003) 2199.
[25] D. Hanson, J. Greenberg, B.E. Henry, E. Kosciuch, Int. J. Mass Spectrom. 223/224 (2003) 507.
[26] A.A. Viggiano, R.A. Morris, F. Dale, J.F. Paulson, J. Chem. Phys. 93 (1990) 1681.
[27] J. de Gouw, C. Warneke, T. Karl, et al., Int. J. Mass Spectrom. 223 (1–3) (2003) 365–382.
[28] Y.K. Lau, S. Ikuta, P. Kebarle, J. Am. Chem. Soc. 104 (1982) 1462.
[29] A.J. Cunningham, J.D. Payzant, P. Kebarle, J. Am. Chem. Soc. 9 (1972) 7627;
H. Ellis, M. Thackston, E. McDaniel, E. Mason, Atom. Nucl. Data Tables 31 (1984) 113.
[30] W. Braun, J.T. Herron, D.K. Kahaner, Int. J. Chem. Kinet. 20 (1988) 51.
[31] H. Takagi, N. Washida, H. Bandow, H. Akimoto, M.J. Okuda, Phys. Chem. 85 (1981) 2701.
[32] D.M. Rowley, P.D. Lightfoot, R. Lesclaux, T.J.J. Wallington, Chem. Soc., Faraday Trans. 87 (1991) 3221.

[33] D.M. Rowley, P.D. Lightfoot, R. Lesclaux, T.J. Wallington, J. Chem. Soc., Faraday Trans. 88 (1992) 1369.
[34] D.M. Rowley, R. Lesclaux, P.D. Lightfoot, B. Nozière, T.J. Wallington, M.D. Hurley, J. Phys. Chem. 96 (1992) 4889.
[35] R. Atkinson, S.M. Aschmann, J. Arey, B.J. Shorees, J. Geophys. Res. 97 (1992) 6065.
[36] M.A. Crawford, J.J. Szente, M.M. Maricq, J.S. Francisco, J. Phys. Chem. A 101 (1997) 5337.
[37] J. Platz, J. Sehested, O.J. Nielsen, T.J. Wallington, J. Phys. Chem. A 103 (1999) 2688.
[38] J.J. Orlando, L. Iraci, G.S. Tyndall, J. Phys. Chem. A 104 (2000) 5072.
[39] R. Atkinson, Int. J. Chem. Kinet. 29 (1997) 99.
[40] R.J. Atkinson, Phys. Chem. Ref. Data Monograph 2 (1994) 1.
[41] J.J. Orlando, G.S. Tyndall, T.J. Wallington, Chem. Rev. 103 (2003) 4657.
[42] R. Atkinson, J. Phys. Chem. Ref. Data 26 (1997) 215.
[43] J. Eberhard, C.J. Howard, J Phys Chem A 101 (1997) 3360.
[44] A. Hansel, A. Wisthaler, Geophys. Res. Lett. 27 (2000) 895.
[45] P.V. Villalta, E.R. Lovejoy, D.R. Hanson, Geophys. Res. Lett. 23 (1996) 1765.